Three-dimensional electric field visualization utilizing electric-field-induced second-harmonic generation in nematic liquid crystals

I-Hsiu Chen, Shi-Wei Chu, Francois Bresson, Ming-Chun Tien, Jin-Wei Shi, and Chi-Kuang Sun

Department of Electrical Engineering and Graduate Institute of Electro-Optical Engineering, National Taiwan University, Taipei 10617, Taiwan

An electric-field-induced second-harmonic-generation signal in a nematic liquid crystal is used to map the electric field in an integrated-circuit-like sample. Since the electric-field-induced second-harmonic-generation signal intensity exhibits a strong dependence on the polarization of the incident laser beam, both the amplitude and the orientation of the electric field vectors can be measured. Combined with scanning second-harmonic-generation microscopy, three-dimensional electric field distribution can be easily visualized with high spatial resolution of the order of 1 μm.   © 2003 Optical Society of America

OCIS codes: 180.6900, 190.4400.

As a result of the widespread use of electronic and optoelectronic devices, the need for an efficient tool to characterize integrated circuits is growing. Electric field sensing is a direct and noninvasive means of performing this kind of characterization. Electron-beam-based systems are widely used but are technically difficult to implement.[1] Thus it is beneficial to find easier alternatives for observing an electric field. Electro-optic (EO) sampling has been widely used to probe electric fields in circuits.[2] However, for one to obtain the distribution of an electric field with EO techniques, the EO crystal needs to scan through the region of interest point by point. Furthermore, the transverse resolution is limited by the size of the probe head ($\sim$10 μm), and the axial resolution is even worse. Utilizing electric-field-induced second-harmonic generation (EFISHG) to probe electric field intensity has recently become an area of interest. The intensity of the EFISHG is proportional to the square of the optical-excitation intensity as well as to the square of the probed electric field magnitude (voltage).[3] Electric fields in different interfaces have been studied with EFISHG effects, including Au/Si,[4] Si/SiO$_2$ heterojunctions,[5] and Au/GaAs Schottky barriers.[6] EFISHG has also been applied to monitoring biomembrane potentials[7] and to mapping the piezoelectric fields in bulk GaN (Ref. 8) and InGaN (Ref. 9) quantum wells with three-dimensional (3D) resolution. Similar to scanning second-harmonic-generation (SHG) microscopy, EFISHG techniques can provide excellent 3D sectioning capability because of the quadratic power dependence.[7] Visualization of a 3D electric field distribution with submicrometer resolution can therefore be achieved. With the help of a fast scanner the focused laser spot can scan across the focal plane at a rate faster than the video rate. Thus direct visualization of real-time images to the electric field can be achieved through a SHG microscope. In this Letter we demonstrate, for the first time to our knowledge, the direct visualization of an electric field through a scanning SHG microscope with the aid of the strong EFISHG effect in a nematic liquid crystal (NLC).

To directly visualize a 3D electric field, we chose a NLC as the SHG active medium for several reasons. First, strong EFISHG has been observed in NLCs.[10–14] Since the EFISHG from a NLC is generated inside the bulk, 3D electric field visualization is achievable; this was not possible in previous interface techniques.[4–6] Second, NLCs are nonconducting and transparent, which allows the fundamental and SHG signals to transmit with minimum attenuation. Third, with a nonprealigned NLC no SHG background from the used bulk NLC can be detected when an electric field is not applied, resulting in a background-free technique. Moreover, for real-time visualization a strong signal is required. The efficiency of the EFISHG effect from NLCs is much higher than that from surfaces and semiconductors, such as GaN. In addition, increasing the excitation light intensity can further enhance the magnitude of the EFISHG signal without increasing the background noise, thus improving the signal-to-noise ratio. Furthermore, the polarization dependence of the EFISHG effect in a nonprealigned NLC allows one to determine the direction of the electric field vector.

Figure 1(A) shows the setup of a scanning SHG microscope.[15] The light source was a Cr:forsterite laser centered at 1230 nm with a 140-fs pulse width and a 350-mW average output power at a 110-MHz repetition rate.[16] The laser was focused onto the sample with a 60$\times$ water-immersion objective (UPLAPO 60$\times$ W/IR, Olympus) with a numerical aperture of 1.2, resulting in a 0.8-μm beam waist radius and an $\sim$0.6-TW/cm^2 peak intensity at the focus. Incorporating an 8-kHz XY scanner (VSH-8, GSI Lumonics) allowed the focused laser spot to scan across the focal plane at more than 40 frames per second. The induced EFISHG image at a wavelength of 615 nm was then projected onto a high-frame-rate CCD camera (Retiga-1350, QImaging) for direct visualization while a color filter was used to remove the fundamental light at 1230 nm. A mirror flipper was placed after the color
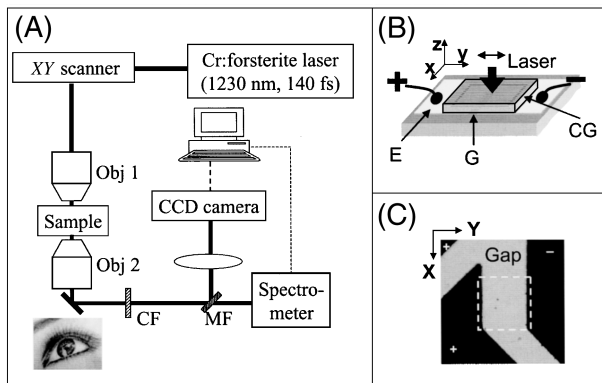
Fig. 1. (A) Setup of a scanning SHG microscope. (B), (C) Detailed sample structure, light path, and orientation convention. Obj, microscope objective; CF, color filter; MF, mirror flipper; E, gold electrode; G, 10-μm groove filled with nonprealigned NLC; CG, microscope cover glass.

filter to select the optical path between the imaging CCD and a spectrometer so that we could perform microspectroscopic measurements at specific points on the samples.

To mimic an integrated circuit, we used the test samples shown in Figs. 1(B) and 1(C). The samples were composed of two gold electrodes (>1 μm thick) on a glass substrate. We put a drop of NLC (E7, Merck Display Technologies) on the 10-μm gap between the two electrodes. A cover glass was then put on the sample to form a flattened NLC layer ($\sim$50 μm thick). In Fig. 1(B) two parallel electrodes are separated by a fixed 10-μm gap to form a uniform electric field. The sample in Fig. 1(C) has a more complicated circuit structure. The samples in Figs. 1(B) and 1(C) differ in only their pattern. To characterize the EFISHG effect in the NLC, we used the sample in Fig. 1(B) for its parallel and uniform electric field. The laser beam was focused onto the middle of the gap with its linear polarization parallel to the electric field. A 615-nm SHG signal was observed in the spectrum immediately. To check whether the signal at 615 nm was EFISHG, the SHG intensity was measured as a function of the applied voltage, which is proportional to the applied field. Figure 2(A) shows the SHG response versus the applied voltage on a log–log scale. The slope of the fitting line is 2.06, showing the square dependence on applied voltage as expected for EFISHG. Since there is no prealignment of the applied NLC, no directional preference is selected by the bulk NLC before applying the electric field as a result of optical centrosymmetry. It is important to note that no SHG can be detected as the applied bias goes to zero (not shown because of the log scale used), indicating a background-free measurement. This also suggests that the instantaneous polarization effect on the boundary layer of the NLC is negligible owing to its weak effect as well as the fact that we are focusing in the bulk rather than in the interfaces. Figure 2(B) shows the dependence of EFISHG intensity on the angle between the electric field and the laser's linear polarization. A sinusoidal response can be observed, which is attributed to the projection of the electric field in the direction

of the pump polarization. As shown in Fig. 2(B), the EFISHG maximum is reached when the polarization is parallel to the static electric field. On the other hand, a minimum that is below the measurement sensitivity is observed when the pump polarization is perpendicular to the electric field. We checked with another polarizer that the polarization of the EFISHG is linear, parallel to the static electric field. According to the orientation convention shown in Fig. 1(B), the dominant component of the EFISHG tensor leading to the observation is $\chi^{(3)}_{yyyy}(2\omega;\omega,\omega,0)$. With linearly polarized light it is possible to determine the electric field vector projected in the xy plane, since EFISHG selects the electric field component parallel to the excitation polarization. By applying two perpendicular excitation polarizations, both the amplitude and the direction of the electric field vector in the xy plane can be obtained. On the other hand, by application of circularly polarized light, the electric field intensity in the xy plane can be obtained with one measurement. After taking the square root of the pixel values of the EFISHG image excited by circularly polarized light, the amplitude of the electric field can be obtained. However, obtaining the direction of the electric field requires two independent measurements.

Figure 3 shows a sectioned image of the amplitude of the electric field projected in the xy plane in the sample from Fig. 1(C). We visualized the electric field components in two perpendicular directions with linearly polarized lights. Figure 3(A) is the sectioned EFISHG image of the electric field component in the $\hat{y} + \hat{x}$ direction (i.e., the laser polarization direction), and Fig. 3(B) is the sectioned EFISHG image of the electric field component in the $\hat{y} - \hat{x}$ direction. Since the original pixel intensities in the CCD array are proportional to the square of the local electric field intensities as shown in Fig. 2(A), we took the square root
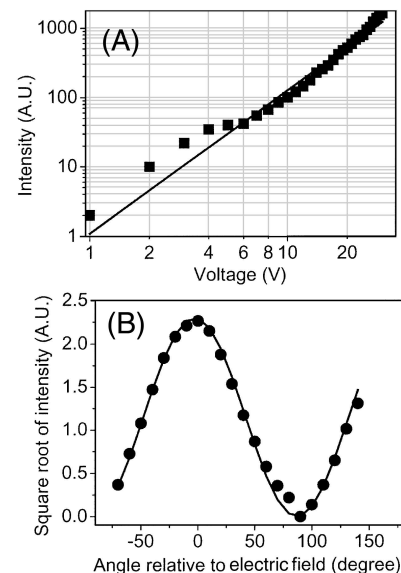

Fig. 2. (A) SHG response versus applied voltage in a log–log scale. The slope of the linear fit is 2.06, indicating its EFISHG nature. (B) SHG response versus excitation light polarization. The maximum occurs when the pump field is parallel to the electric field.
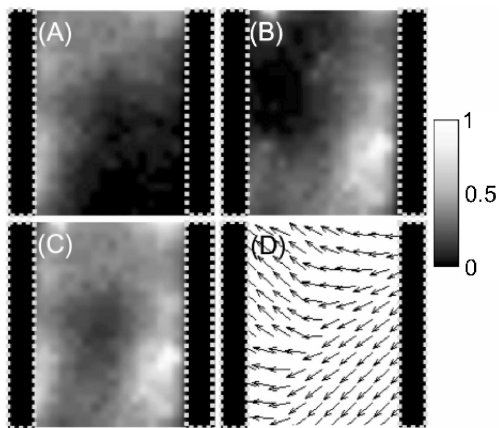
Fig. 3. Imaged electric field vector distribution in the plane of the electrode within the squared region of Fig. 1(C). (A) Sectioned image measuring the electric field component in the direction of $\hat{y} + \hat{x}$. (B) Sectioned image measuring the electric field component in the direction of $\hat{y} - \hat{x}$. (C), (D) Recovered amplitude and direction of the electric field vector, respectively. Image size: 12×12 μm.

of the CCD pixel intensities in Figs. 3(A) and 3(B). A fixed 25-V dc bias was applied to the sample during the measurement. To obtain the electric field amplitude distribution in the xy plane [Fig. 3(C)], we added the intensity value (rather than the square root of the value) of each pixel in Figs. 3(A) and 3(B) and then took the square root. On the other hand, to obtain the directions of the electric field vectors, the amplitude of one electric field component was divided by the value of the corresponding pixel in the other sectioned image. The angle θ between the electric field and the polarization was then calculated from the quotient q with $\tan \theta = q$. However, there was an ambiguity in determining θ because we could not distinguish θ from $(\pi - \theta)$ since only the absolute values of the electric field components were measured. To overcome this ambiguity, an extra single-point measurement was applied with a third laser polarization. Figure 3(D) shows the recovered electric field direction in the xy plane. We also studied the electric field distribution at different heights and obtained excellent z resolution of the order of 1 μm (not shown).

Although the electric field vector projected in the xy plane can be measured with 3D resolution, the z component of the electric field component was not obtained in the above demonstration. As previously mentioned, EFISHG occurs when the polarization of the incident beam is parallel to the electric field. As a result, only the electric field in the xy plane is measured if light propagates in the z direction. To obtain the z compo-

nent of the electric field, one has to tilt the sample or adjust the direction of the excitation light. Three independent measurements are required to fully recover the total electric field magnitude and direction in 3D spaces.

In summary, direct electric field visualization was achieved with a scanning SHG microscope utilizing the EFISHG effect in a NLC. Taking advantage of the nonlinear effect, excellent 3D resolution of the order of less than 1 μm can be achieved. Since the EFISHG signal intensity is dependent on the polarization of the incident laser beam, the amplitude and orientation of the electric field vectors can all be measured.

References

1. E. Menzel and E. Kudalek, Scanning **5,** 103 (1983).
2. K. J. Weingarten, M. J. W. Rodwell, and D. M. Bloom, IEEE J. Quantum Electron. **24,** 198 (1988).
3. C. H. Lee, R. K. Chang, and N. Bloembergen, Phys. Rev. Lett. **18,** 167 (1967).
4. C. Ohlhoff, C. Meyer, G. Lupke, T. Loffler, T. Pfeifer, H. G. Roskos, and H. Kurz, Appl. Phys. Lett. **68,** 1699 (1996).
5. J. I. Dadap, X. F. Hu, M. H. Anderson, M. C. Downer, J. K. Lowell, and O. A. Aktsipetrov, Phys. Rev. B **53,** 7607 (1996).
6. W. de Jong, A. F. Etteger, C. A. van't Hof, P. J. van Hall, and T. Rasing, Surf. Sci. **331–333,** 1372 (1995).
7. G. Peleg, A. Lewis, M. Linial, and L. M. Loew, Proc. Natl. Acad. Sci. USA **96,** 6700 (1999).
8. C.-K. Sun, S.-W. Chu, S.-P. Tai, S. Keller, U. K. Mishra, and S. P. DenBaars, Appl. Phys. Lett. **77,** 2331 (2000).
9. C.-K. Sun, S.-W. Chu, S. P. Tai, S. Keller, U. K. Mishra, and S. P. DenBaars, Scanning **23,** 182 (2001).
10. M. I. Barnik, L. M. Blinov, A. M. Dorozhkin, and N. M. Shtykov, Mol. Cryst. Liq. Cryst. **98,** 1 (1983).
11. N. V. Tabiryan, A. V. Sukhov, and B. Y. Zeldovich, Mol. Cryst. Liq. Cryst. **136,** 1 (1986).
12. S. D. Durbin, S. M. Arakelian, and Y. R. Shen, Phys. Rev. Lett. **47,** 1411 (1981).
13. S. K. Saha and G. K. Wong, Appl. Phys. Lett. **34,** 423 (1979).
14. R. Stolle, T. Dürr, and G. Marowsky, J. Opt. Soc. Am. B **14,** 1583 (1997).
15. For future applications a point-by-point mapping photomultiplier-tube-based reflection-type scanning SHG microscope could be used. The forward emitted SHG signal would be reflected by the device surface and could be detected with a photomultiplier tube.
16. T.-M. Liu, S.-W. Chu, C.-K. Sun, B.-L. Lin, P.-C. Cheng, and I. Johnson, Scanning **23,** 249 (2001).